Journal of Molecular Graphics and Modelling 27 (2008) 332–341

Contents lists available at ScienceDirect

Journal of Molecular Graphics and Modelling

journal homepage: www.elsevier.com/locate/JMGM

Functional and structural characterization of PKA-mediated pH_i gating of ROMK1 channels

Chien-Hsing Lee [a,1], Po-Tsang Huang [b,c,1], Kuo-Long Lou [b,c,*], Horng-Huei Liou [a,d,**]

[a] Department of Pharmacology, College of Medicine, National Taiwan University, Taiwan
[b] Institute of Biochemistry and Molecular Biology, College of Medicine, National Taiwan University, Taiwan
[c] Graduate Institute of Oral Biology, Medical College, National Taiwan University, Taiwan
[d] Department of Neurology, National Taiwan University Hospital, Taipei, Taiwan

ARTICLE INFO

Article history:
Received 29 February 2008
Received in revised form 26 May 2008
Accepted 2 June 2008
Available online 8 June 2008

Keywords:
HPS/aBS
Homology model
Molecular dynamics simulations
pH_i
PKA
ROMK1 channels

ABSTRACT

Hyperprostaglandin E syndrome/antenatal Bartter syndrome (HPS/aBS) is a severe salt-losing renal tubular disorder and results from the mutation of renal outer medullary K^+ (ROMK1) channels. The aberrant ROMK1 function induces alterations in intracellular pH (pH_i) gating under physiological conditions. We investigate the role of protein kinase A (PKA) in the pH_i gating of ROMK1 channels. Using giant patch clamp with *Xenopus* oocytes expressing wild-type and mutant ROMK1 channels, PKA-mediated phosphorylation decreased the sensitivity of ROMK1 channels to pH_i. A homology model of ROMK1 reveals that a PKA phosphorylation site (S219) is spatially juxtaposed to the phosphatidylinositol 4,5-bisphosphate (PIP_2) binding residues (R188, R217, and K218). Molecular dynamics simulations suggest a stable transition state, in which the shortening of distance between S219 and R217 and the movement of K218 towards the membrane after the PKA-phosphorylation can be observed. Such conformational change may bring the PIP_2 binding residues (K218) more accessible to the membrane-bound PIP_2. In addition, PIP_2 dose-dependently reactivates the acidification-induced rundown channels only when ROMK1 channels have been phosphorylated by PKA. This implies a sequence regulatory episode reflecting the role of PIP_2 in the pH_i gating of ROMK1 channels by PKA-mediated phosphorylation. Our results provide new insights into the molecular mechanisms underlying the ROMK1 channel regulation associated with HPS/aBS.

1. Introduction

The family of inwardly rectifying K^+ (Kir) channels is composed of seven different subfamilies, Kir1–Kir7 [1]. All Kir channels are tetrameric and contain two transmembrane helix domains (TM1 and TM2), the ion-selective pore-loop, and cytoplasmic N- and C-terminal domains. The renal outer medullary K^+ (ROMK1; Kir1.1) channels are unique among Kir channel members in showing an exquisite sensitivity to intracellular protons (pH_i) [2]. This reduction in K^+ conductance by acidification plays a key role in K^+ homeostasis during metabolic acidosis. The cDNAs for ROMK1 and its isoforms ROMK2 and ROMK3 have been isolated [3]. ROMK1 encodes a 391 amino acids polypeptide. ROMK2 encodes a 372 amino acids polypeptide that lacks the first 19 amino acids of ROMK1, but is otherwise identical to ROMK1. ROMK3 encodes a 399 amino acid polypeptide that has a unique sequence for the first 19 amino acids in the N-terminus. N-terminal splice variants of ROMK isoforms have similar primary structure and are responsible for potassium ion efflux in the kidney [2].

Aberrant activity of Kir channels has been linked to a variety of endocrine, cardiac, and neurological disorders [4–6]. The hyperprostaglandin E syndrome/antenatal Bartter syndrome (HPS/aBS) results from the inherited mutations in ROMK1 channels [7], characterized by natriuresis, diuresis, hypokalemic metabolic alkalosis and elevated prostaglandin E_2. Analysis of the ROMK1 gene in individual HPS/aBS patients identified a number of point mutations in the core region as well as in the intracellular N- and C-terminus [8]. Mutations in cytoplasmic domains cause a shift of the pH_i gating [9]. The pH_i gating process has been reported to involve a large number of protein domains and amino acid residues in the intracellular N- and C-terminus [10]. Protonations of several

* Corresponding author at: Graduate Institute of Oral Biology College of Medicine, National Taiwan University, No 1, Chang-Teh Street, Taipei 100, Taiwan. Tel.: +886 2 23123456x6611; fax: +886 2 23820785.
** Corresponding author at: Department of Pharmacology and Neurology, College of Medicine, National Taiwan University, Room 1141, No 1, Sec 1, Jan-Ai Road, Taipei 100, Taiwan. Tel.: +886 2 23123456x8325; fax: +886 2 23915297.
E-mail addresses: kllou@ntumc.org (K.-L. Lou), hhl@ntu.edu.tw (H.-H. Liou).
[1] These authors are equally contributed to this work.

1093-3263/$ – see front matter © 2008 Elsevier Inc. All rights reserved.
doi:10.1016/j.jmgm.2008.06.001

residues in the C-terminus initiate the movements of N–C-terminus, producing vast conformational changes in the channel protein, and then closes the channels [11,12], suggesting that pH_i gating process induces a global conformational change in ROMK1 channels.

Many of the mutations in ROMK1 channels related to HPS/aBS have been found close to the cAMP-dependent protein kinase (PKA)-mediated phosphorylation sites, being S44, S219, and S313 [13,14]. The S219 mutations have been observed on HPS/aBS [15,16]. The PKA site mutations of ROMK2 channels shift the pH-dependence to more alkaline values [17], implying that the pH_i gating of ROMK channels modulated by PKA. The molecular mechanism of PKA-mediated phosphorylation in regulating the pH_i sensitivity of ROMK channels remains unclear. As suggested earlier, the PKA-mediated phosphorylation modulates K_{ATP} channel activity through a structural change in protein [18]. This observation arouses the consideration or a hypothesis that PKA-mediated phosphorylation may affect pH_i gating through inducing conformational changes.

The molecular dynamics (MD) simulation provided valuable insights in the regulation mechanisms in different ionic channels (such as the nicotinic receptor and the Kir channel) under conditions that are difficult to achieve with electrophysiological experimental techniques [19,20]. Based on the X-ray crystal structure of KirBac1.1 [21], we investigate the cytoplasmic part of ROMK1 channels by means of MD simulations, to provide a description of the molecular process driven by PKA leading to the pH_i gating of channels. Our results suggested the structural and functional roles of PKA-mediated phosphorylation in regulating the pH_i sensitivity of ROMK1 channels, by inducing a conformation change that shortens the distance between S219 and R217 as well as the distance between the phosphatidylinositol 4,5-bisphosphate (PIP_2)-binding residues and membrane.

2. Materials and methods

2.1. Molecular biology

Site-directed mutagenesis was performed using a commercial mutagenesis kit (Stratagene Co.) and confirmed by nucleotide sequencing as described previously [22]. mCAP RNAs of the wild-type and mutant channels were *in vitro* transcribed using T7 RNA polymerase (Ambion Co.) [22,23].

2.2. Oocytes preparation and injection

Female *Xenopus laevis* frogs were briefly anesthetized by immersion in 0.1% 3-aminobenzoic acid ethyl ester and a few lobes of the ovaries removed after a small abdominal incision. The incision was sutured and the frogs were allowed to revive after surgery [24]. The oocytes were incubated for 90 min at room temperature (23–25 °C) with 2 mg/ml of collagenase (Type I, Sigma Chemicals.) in OR_2 solution consisting of (in mM) 82 NaCl, 2 KCl, 1 $MgCl_2$, and 5 HEPES, pH 7.4, to remove the follicular layer. After 10 washes with OR_2 solution, oocytes at Dumont stage V–VI were selected and injected with 30 ng of mRNA, then incubated at 18 °C in ND96 solution consisting of (in mM) 96 NaCl, 2 KCl, 1 $MgCl_2$, 1.8 $CaCl_2$, 5 HEPES, pH 7.5, supplemented with 100 mg/l of penicillin-streptomycin and 10 mg/ml of geneticin. Channel activity was assessed 3 days post-injection.

2.3. Giant patch-clamp recording

Xenopus oocytes were injected with wild-type or mutant ROMK1 mRNA and giant patch-clamp recording performed as described previously [22,23,25]. The pipette (extracellular) solution contained (in mM) 100 KCl, 2 $CaCl_2$, and 5 HEPES, pH 7.4, while the bath (cytoplasmic) solution contained either 100 KCl, 5 HEPES, 5 EGTA, and 1 $MgCl_2$ (pH 7.4) (Mg^{2+} solution) or 100 KCl, 5 HEPES, 5 EDTA, 4 NaF, 3 Na_3VO_4, and 10 $Na_4P_2O_7$ (FVPP solution) as indicated for each experiment. Inward K^+ currents (at a −60 mV holding potential at 23–25 °C) were recorded on a chart recorder using an Axopatch 200B amplifier (Axon Instruments, Foster City, CA) and the recorder strips scanned and analyzed on a computer. All the data were expressed as the mean ± standard error of the mean.

$$\sigma_M = \frac{\sigma}{\sqrt{N}}$$

where σ is the standard deviation of the original distribution and N is the sample size (the number of scores each mean is based upon).

2.4. Drug treatment and administration

PIP_2 (Boehringer Mannheim) was diluted in water (1 mg/ml) and sonicated to form liposomes [23]. A stock solution of PKA catalytic subunit (Sigma, 2000 units/ml dissolved in water containing 40 mM DTT) was diluted 20-fold in experimental solutions to yield final concentrations of 100 units/ml of PKA and 2 mM DTT.

2.5. Homology modeling of ROMK1

2.5.1. Search for templates

The bell laboratory layered space-time algorithm was used to search the protein data bank (PDB) for protein segments with sequences similar to those of ROMK1 (Genbank accession number P48048) and structures which could serve as viable structural templates. The mammalian Kir channel has recently been advanced by X-ray crystal structures of the prokaryotic homolog (KirBac1.1) [21]. KirBac1.1, a prokaryotic ortholog of ROMK, has suggested that channel pH_i gating involves intermolecular interactions of the N- and C-terminal domains of adjacent subunits [12]. The crystal structures of the KirBac1.1 template sequence that showed the highest scores in the homologus sequence alignment were chosen for the determination of structure conserved regions (SCRs). The sequence identity between ROMK1 channels and KirBac1.1 is 30%, whereas the similarity between them is 60%. They indeed belong to the same family, both in structure and in function.

2.5.2. Paired sequence alignment

The European Molecular Biology Open Software suite program was used to determine equivalent residues in KirBac1.1 and ROMK1 channels. The amino acid sequence of ROMK1 was then included in the multiple sequence alignment of the appropriate template regions to specify the residue numbers for model building.

2.5.3. Model building and residue side chain simulation

Homology modeling was performed following previously described procedures [26–28]. Briefly, the residues of the ROMK1 channel chosen according to the results of GCG paired sequence alignment were superimposed onto the structure coordinates of the C_α atoms of the corresponding SCRs from the template channel structure (PDB ID: 1P7B). This generated the secondary structure and relative positions of the definite structural elements in the chosen residues of the ROMK1 model. Junctions between secondary structural elements were determined according to the 10 choices provided by software (Insight II model, Accelrys Inc., San Diego, CA). We chose the loop with the lowest energies and root mean square deviations (RMSD), in combination with slight

manual adjustments, if short contacts were observed. After all the operation is accomplished, overall energy minimization was performed again to obtain the final model. Hydrophobic/hydrophilic interactions between residue side chains were observed from the model to provide required structural–functional interpretation. All calculations and structure manipulations were performed using the Discover/Insight II molecular simulation and modeling program (Accelrys Inc., San Diego, CA; release 950) on Silicon Graphics Octane/SSE and O2/R12000 workstations and an O-300 server.

2.5.4. Molecular dynamics simulations

MD simulations were performed using InsightII 2005 and the chemistry at HARvard molecular mechanics 27b4 forcefield [29]. The system is in an appropriate environment with the TIP3P water model. Additional counterions were added so that the overall net charge on the system was zero. The final system consisted of ~100,000 atoms. During this equilibration process, the water molecules and ions were free to move. The parameter employed to set up the simulation were in use of Berendsen coupling to maintain a constant temperature of 300 K and a constant pressure

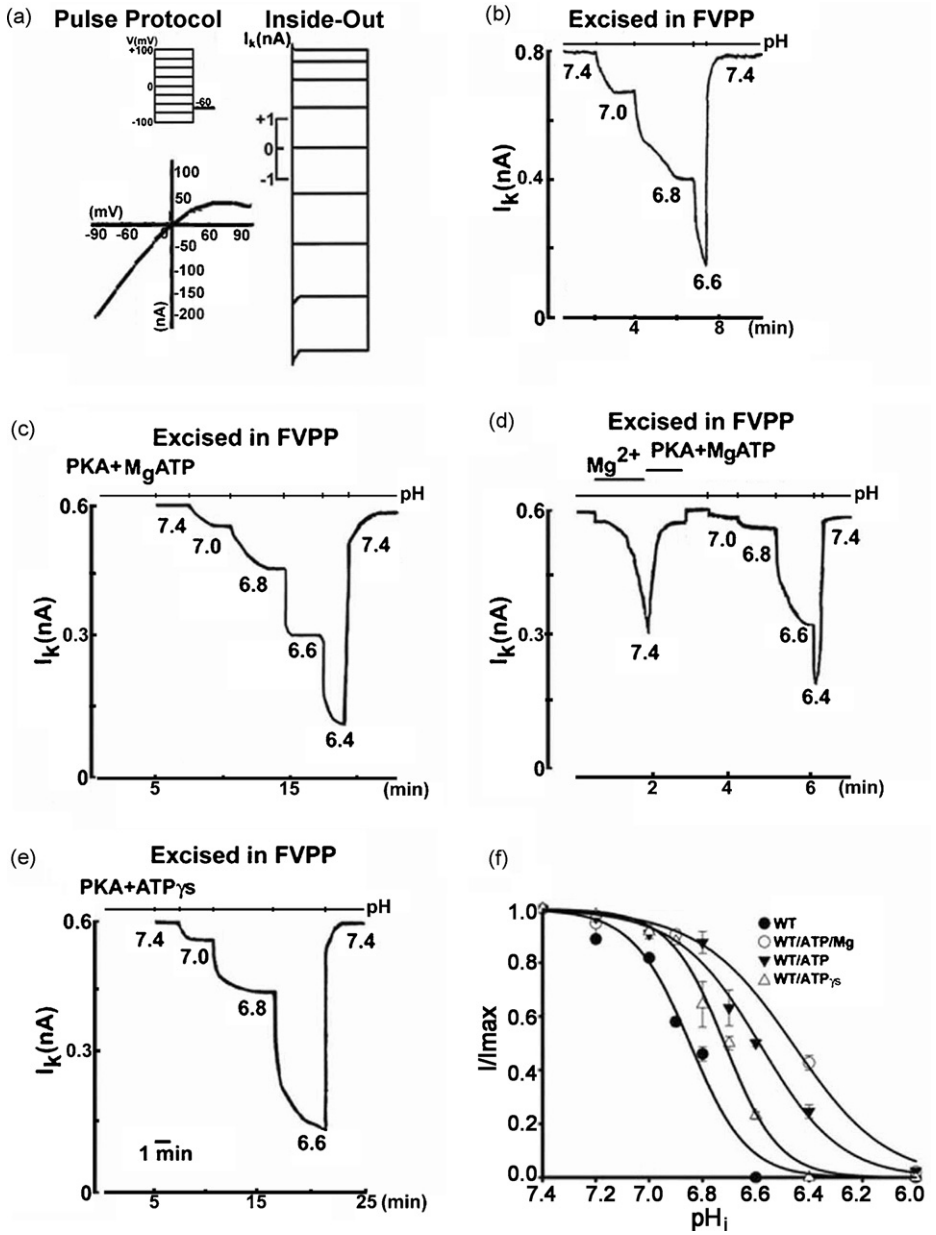

Fig. 1. Effects of PKA-mediated phosphorylation on pH_i gating in ROMK1 channels. ROMK1 channels were expressed in *Xenopus* oocytes and the K^+ currents (I_k) recorded in on-cell, giant patches, which were then excised into the FVPP solution. Voltage pulses were applied from −100 to +100 mV at 25 mV increments. The holding potential was −60 mV. (a) ROMK1 channels showed an inwardly rectifying pattern. (b) The excised patches of ROMK1 channel current titrated to the intracellular pH (pH_i) value (from 7.4 to 6.6), currents were inhibited by progressively more acidic pH_i. After inhibition, membrane patches were alkalinized to pH_i 7.4 to assess the level of remaining currents. (c) Pre-treatment of PKA catalytic subunit (100 units/ml) and Mg-ATP (0.5 mM) for 5 min, the acidification resulted in a steep pH-dependent inhibition with a effective acidic dissociation constant (pK_a) of 6.64 ± 0.02 (n = 5, $P < 0.05$). (d) Mg^{2+}-containing solution induces rundown of inside-out ROMK1 channel patches and the application of PKA catalytic subunit (100 units/ml) and MgATP (0.5 mM) reactivates these channels. Acidification of rundown channels revealed a pK_a of 6.58 ± 0.02 (n = 5). (e) Pre-treated with PKA catalytic subunit (100 units/ml) and ATP[γS] (0.5 mM) for 5 min, the acidification caused a pH-dependent inhibition with a pK_a of 6.72 ± 0.01 (n = 5). This pK_a was not significantly different from that of channels phosphorylated by PKA and MgATP. (f) Comparison the pH_i dependent inhibition of the ROMK1 channels and PKA-mediated phosphorylation ROMK1 channels. The relative currents [%; normalized to the maximal currents (I_{max}) at pH_i 7.4] at different pH_i values were fitted to the Hill equation.

of 1 bar. Van der Waals interactions were modeled using a 6–12 (or Lennard Jones, L-J) potential with a cutoff value of 12 Å. The particle-meshed Ewalds method [30] was used to identify long-range electrostatic interactions with a cutoff of 12 Å. The linear constraint solver algorithm was used to constrain the covalent bonds [31].

3. Results

3.1. Effects of PKA-mediated phosphorylation on pH_i gating in ROMK1 channels

ROMK1 channels were expressed in *Xenopus* oocytes and the K^+ currents recorded in on-cell, giant patches, which were then excised into Mg^{2+}-free bath solution containing a mixture of phosphatase inhibitors, fluoride, vanadate, and pyrophosphate (FVPP solution). This solution prevents run-down of the ROMK1 current, probably by inhibiting both Mg^{2+}-dependent protein phosphatases and lipid phosphatases, thus slowing channel dephosphorylation and membrane PIP_2 depletion [22,23,32]. The activity of wild-type channels at pH_i 7.4 (measured as the inward K^+ current at a −60 mV holding potential, Fig. 1a) was near maximal in the on-cell patches and was increased by less than 10% when the cytoplasmic face of the excised inside-out membrane patches was alkalinized to pH_i 9.4 (data not shown). Subsequent acidification inhibited the current in a steep pH_i-dependent manner. The effective acidic dissociation constant (pK_a) for inhibition of ROMK1 channels by intracellular acidification was 6.86 ± 0.05 (n = 5; Fig. 1b and f).

MgATP not only serves as the substrate for the PKA catalytic subunit, but also activates lipid kinases to generate PIP_2 [23]. Pretreatment of inside-out patches containing ROMK1 channels with PKA catalytic subunit and Mg-ATP for 5 min followed by subsequent acidification resulted in a steep pH-dependent inhibition with a pK_a of 6.64 ± 0.02 (n = 5). The pK_a of the ROMK1 channels shifted to a more acidic value in the PKA-phosphorylated channels than in those not subjected to PKA treatment ($P < 0.05$; Fig. 1c and f) and this process may be dependent on the PIP_2 interaction. Mg^{2+}-containing solution induces rundown of inside-out ROMK1 channel patches and application of PKA catalytic subunit and MgATP reactivates these channels [23]. Acidification of these channels revealed a pK_a of 6.58 ± 0.02 (n = 5; Fig. 1d and f), which is similar to that for channels pre-incubated with PKA catalytic subunit and MgATP. ATP[γS] can also serve as a substrate for PKA [33], but without activating lipid kinases to produce PIP_2 [23]. When inside-out patches were pre-treated with PKA catalytic subunit and ATP[γS] for 5 min, intracellular acidity caused a steep pH-dependent inhibition of the ROMK1 channel, with a pK_a of 6.72 ± 0.01 (n = 5; Fig. 1e and f). This pK_a was not significantly different from that of channels phosphorylated by PKA and MgATP. These results suggest that PKA-mediated phosphorylation affects the pH_i sensitivity of ROMK1 channels, shifting the pK_a towards more acidic values.

3.2. Effects of mutation of PKA sites on pH_i gating

K80 in the N-terminal regions of ROMK1 channels plays an important role in pH_i regulation [34,35]. When K80 was mutated to methionine, the pK_a of the K80M mutant channel was 6.01 ± 0.03 (n = 5; Fig. 2a and d) compared to the value of 6.86 for the wild-type. To investigate the role of residues at the PKA phosphorylation sites in the regulation of pH_i gating when K80 was mutated, two double mutants, K80M/S219A and K80M/S313A, were constructed and their

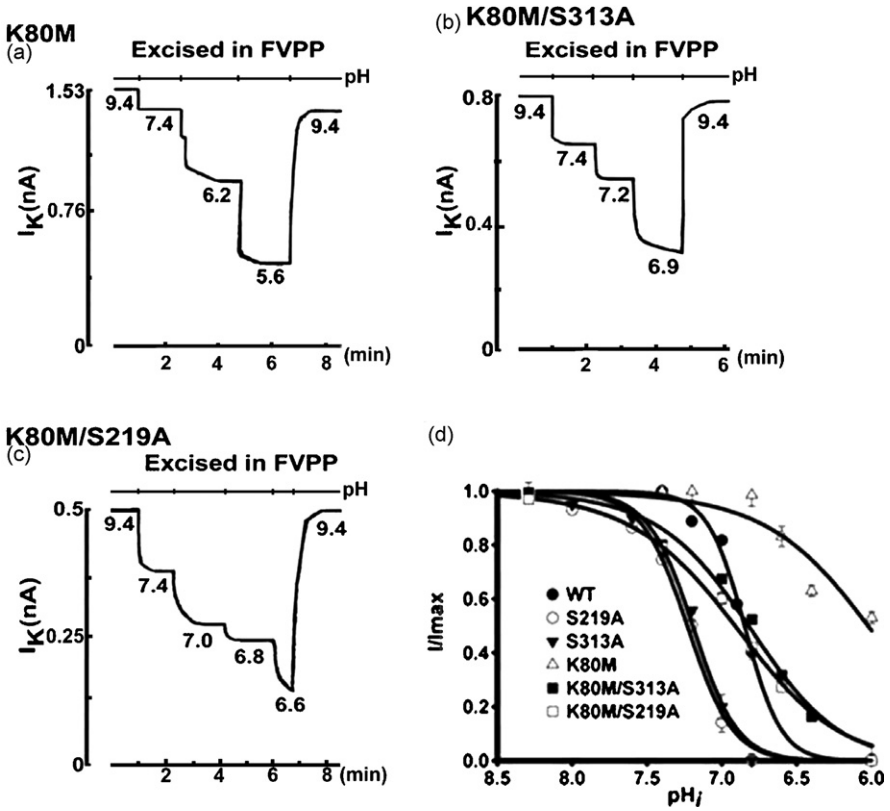

Fig. 2. Effects of mutations at K80 and PKA phosphorylation sites in ROMK1 channels on pH_i gating. (a) The pK_a for K80M mutant channels was 6.01 ± 0.03 (n = 5). (b) The pK_a for K80M/S219A mutant channels was 6.92 ± 0.01 (n = 5). (c) The pK_a for K80M/S313A mutant channels was 6.81 ± 0.01 (n = 5). (d) Comparison of the pH_i response curves for the wild-type and mutated ROMK1 channels.

pK_a values were found to be similar to that of the wild-type ROMK1 channel (6.92 ± 0.01, $n = 5$, and 6.81 ± 0.01, $n = 5$, respectively; Fig. 2b and c). The double mutants (K80M/S219A and K80M/S313A) revealed that the K80 mutation and the S219 or S313 mutation shifted the pK_a in an additive fashion. These results indicate that PKA and K80 mediate the pH_i gating process by independent mechanisms.

A previous report [14] suggested that three serine residues are important in the PKA-mediated phosphorylation of ROMK1 channels, these being S44 in the N-terminal and S219 and S313 in the C-terminal cytoplasmic domains. Single mutation of S219 or S313 (but not S44) to alanine reduces the single channel open probability by ~50% [36]. Our data showed that the pK_a for S219A and S313A was shifted in the alkaline direction (7.28 ± 0.04, $n = 5$ and 7.24 ± 0.02, $n = 5$, respectively; Fig. 3b and c). Mutation of the PKA target sites S219 and S313 to aspartate mimics the negative charge carried by a phosphate group bound to a serine. This pK_a for S219D and S313D was (8.02 ± 0.03, $n = 6$ and 7.16 ± 0.02, $n = 6$, respectively; Fig. 3d and e).

3.3. Structural analysis of ROMK1 channels phosphorylation

To better understand these findings from a structural perspective, we employed a combination of homology modeling and MD simulations. Fig. 4a shows the comparison of the sequences of ROMK1 channels and the closely related KirBac1.1 channels. Sequence identity and similarity between the KirBac1.1 and ROMK1 channels is around 30% and 60%, respectively. Residues 62–329 in the ROMK1 channel sequence were aligned with residues 41–309 of the KirBac1.1 sequence for homology modeling. Sequence identities for residues in N-terminal domains (62–76 in ROMK1 and 41–53 in KirBac1.1), TM1 (77–120 in ROMK1 and 54–88 in KirBac1.1), pore domains (121–153 in ROMK1 and 89–124 in KirBac1.1), TM2 (154–175 in ROMK1 and 125–142 in KirBac1.1) and C-terminal domains (176–329 in ROMK1 and 143–289 in KirBac1.1) are 37.5%, 34.1%, 48.4%, 48%, and 35.7%, respectively. Meanwhile, the corresponding sequence similarities based on the above comparisons are 62.5%, 63.6%, 75.7%, 80% and 63.5%, respectively.

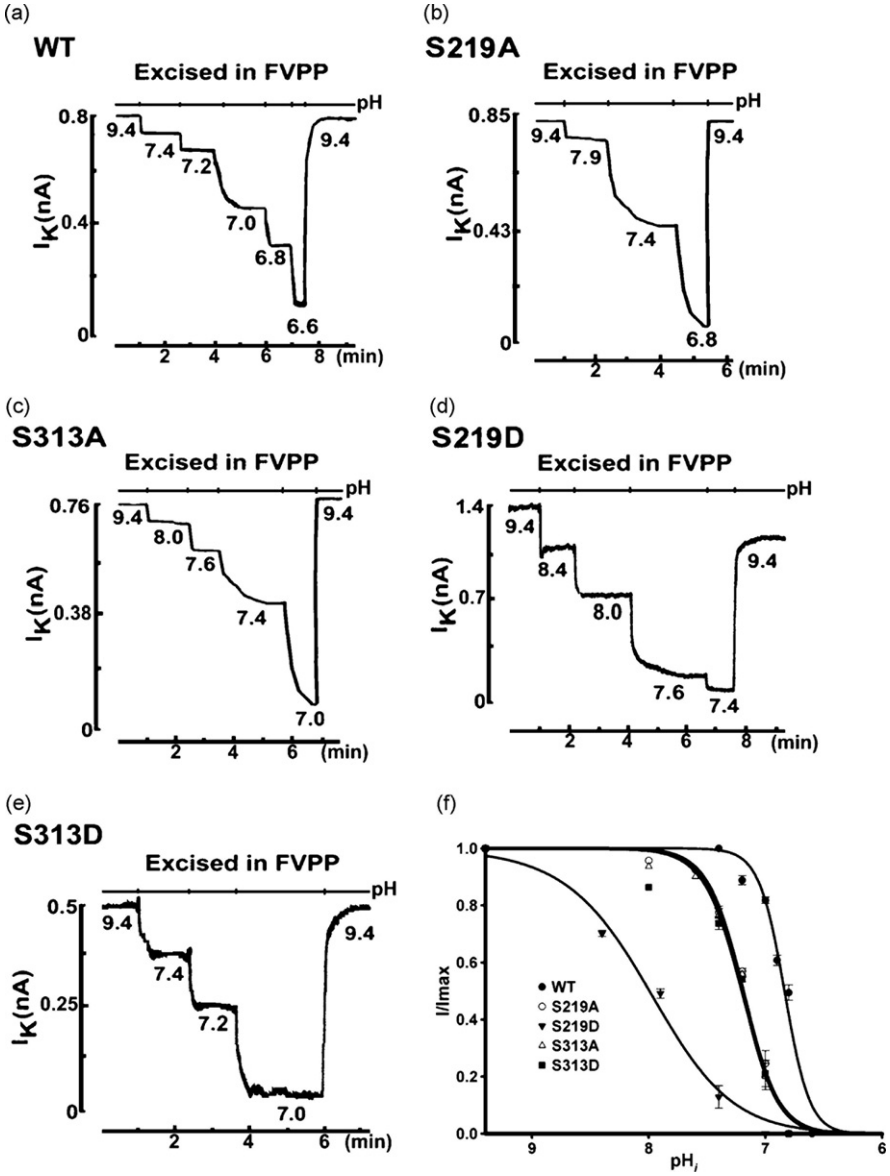

Fig. 3. Effects of mutation of PKA sites on pH_i gating. (a) The pK_a for inhibition of wild-type ROMK1 channels (WT) by intracellular acidification was 6.86 ± 0.05 ($n = 6$). (b) The pK_a for S219A mutant channels was 7.28 ± 0.04 ($n = 5$). (c) The pK_a for S313A mutant channels was 7.24 ± 0.02 ($n = 5$). (d) The pK_a for S219D mutant channels was 8.02 ± 0.03 ($n = 6$). (e) The pK_a for S313D mutant channels was 7.16 ± 0.02 ($n = 6$). (f) Comparison of the pH_i response curves for the wild-type and PKA mutated ROMK1 channels.

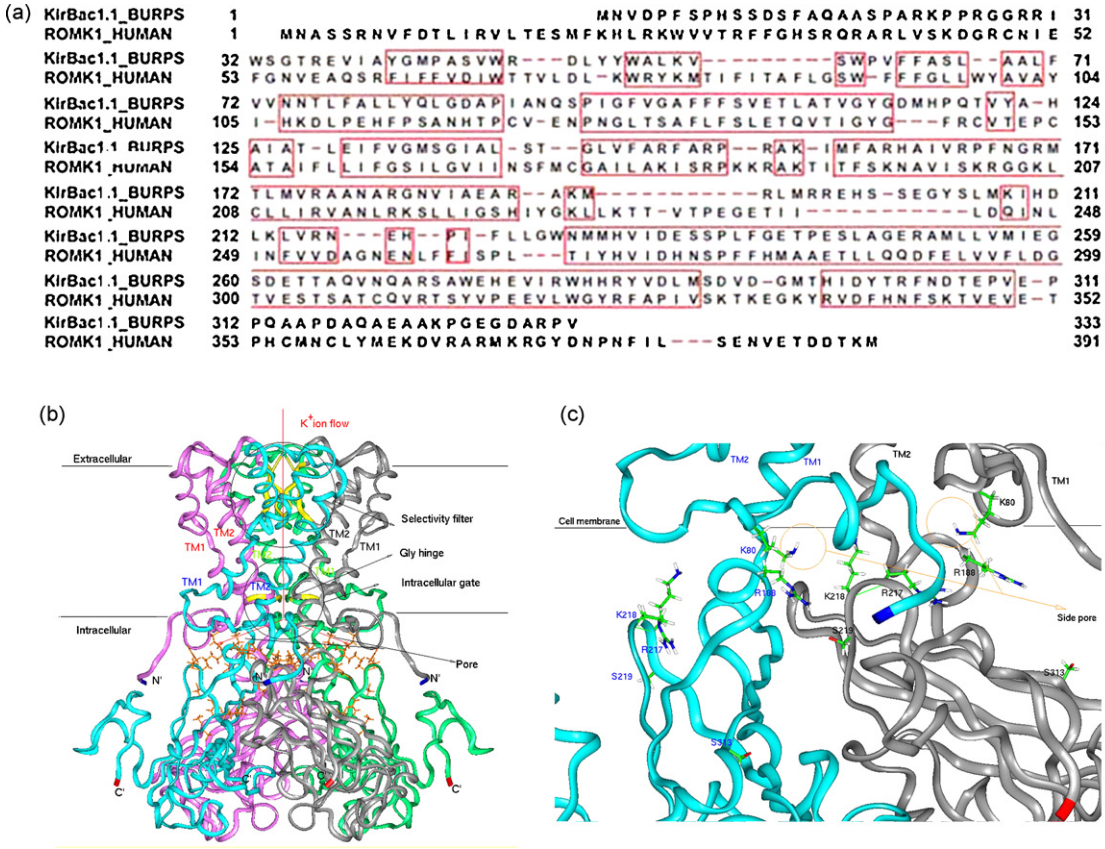

Fig. 4. The construction of a molecular model of ROMK1 channels. (a) Sequence alignment of KirBac1.1 (PDB code: 1P7B) and ROMK1 (Swissprot ID: P48048). Residues 61–329 in the ROMK1 sequence were aligned with residues 36–309 in the KirBac1.1 sequence. Structural conserved regions (SCRs) are boxed in red. The coordinates of the C_α atoms in template proteins (KirBac1.1) were used to build up the ROMK1 channel model framework (C_α atom trace). Gaps between two SCRs were filled with loops generated from a loop database. (b) Overall structure of the ROMK1 tetrameric model. The main chains of the four subunits are represented with ribbons in different colors, the N- and C-terminus being marked in blue and red, respectively. Important motifs, such as two membrane-spanning α-helices, the selectivity filter, glycine hinge, intracellular gate, and the channel pore, and the direction of potassium flow are emphasized with arrows. The side-chains of crucial basic residues discussed in the text are shown as orange sticks. (c) Spatial organization of the crucial basic residues. For better viewing, two subunits of the tetramer have been removed from the structure. Residue side-chains are depicted in different colors according to their atom types. K80 in the N-terminal domains is fairly close to the intracellular channel gate, while the PKA phosphorylation site, S219, is in the C-terminal domains and close to the PIP_2 binding residues, R188, R217, and K218.

Fig. 4b shows the homology model of the ROMK1 channels based on the crystal structure of the KirBac1.1 channel [21]. The important motifs, such as pore helices and selective filter are located at pore domains and the glycine hinges are located on the end of TM2. The TM domains of the tetrameric ROMK1 channels structure consist of TM1 and TM2 per subunit (Fig. 4b). For the intracellular domains, several crucial structural features are emphasized with residue numbers indicated. For example, K80 in the N-terminal domains is fairly close to the intracellular channel gate, whereas the PKA phosphorylation site, S219, is located in the C-terminal domains and juxtaposed to the PIP_2 binding site residues, R188, R217, and K218 (Fig. 4c).

MD simulations suggested that PKA-mediated phosphorylation results in differences in the total root RMSD and in the total energy of ROMK1 structures. This new conformation may reflect a relatively more stable transition state (Fig. 5a). For the interaction occurring at the phosphorylation sites, Fig. 5b indicates both a stable conformation after the phosphorylation and the new distance formed at the tips of side chains between S219 and R217, for which it decreases from 10 Å to 3–5 Å. In comparison, the distance between S219 and K218 increases from 8 Å to 12–13 Å (Fig. 5c).

3.4. Sequence effects of PKA-mediated phosphorylation and the PIP_2-channel interaction on pH_i gating of channels

We investigate the role of PIP_2 in the PKA-mediated phosphorylation on the pH_i sensitivity of ROMK1 channels. The rate of channels decline caused by anti-PIP_2 antibodies represents the channel-PIP_2 interaction. A more rapid inhibition rate indicated a rather weak PIP_2-channel interaction [22,23]. At pH_i 6.8, the ROMK1 channel was inhibited by application of anti-PIP_2 antibodies with a $t_{1/2}$ of 45 ± 3 s ($n = 4$), significantly faster than PKA-phosphorylated channels ($t_{1/2} = 60 \pm 3$ s, $n = 4$, $P < 0.05$; Fig. 6a). Thus, PKA-mediated phosphorylation of ROMK1 enhances the PIP_2-channel interaction in acidic conditions.

As shown in Fig. 6b, PIP_2 (50 μM) alone cannot rescue the channel currents during the rapid acidification (from pH_i 9.4 to 6.4). Whereas, inside-out excised patches containing ROMK1 channels were pre-treated with PKA catalytic subunit and ATP[γS], the pH_i-dependent inhibition caused by intracellular acidification (pH_i 9.4–6.4) was fully recovered by replacement of the bath solution with one containing 50 μM PIP_2 in the form of liposomes (Fig. 6c). Fig. 6d and e shows that the inhibition caused by intracellular protons (pH_i 7.4–6.8) was overcome by PIP_2 in a dose-dependent manner only in those channels have been phosphorylated by PKA. Both 10 and 50 μM (but not 5 μM) PIP_2 completely reactivated the rundown channels caused by pre-treatment with PKA catalytic subunit and ATP[γS], although the reactivation with 10 μM PIP_2 was much slower than that with 50 μM PIP_2 (Fig. 6d). In contrast, without pretreatment with PKA catalytic subunit and ATP[γS], none of the three concentrations of PIP_2 reactivated rundown channels (Fig. 6e). These results imply a sequence regulatory mechanism in which PKA-mediated phosphorylation

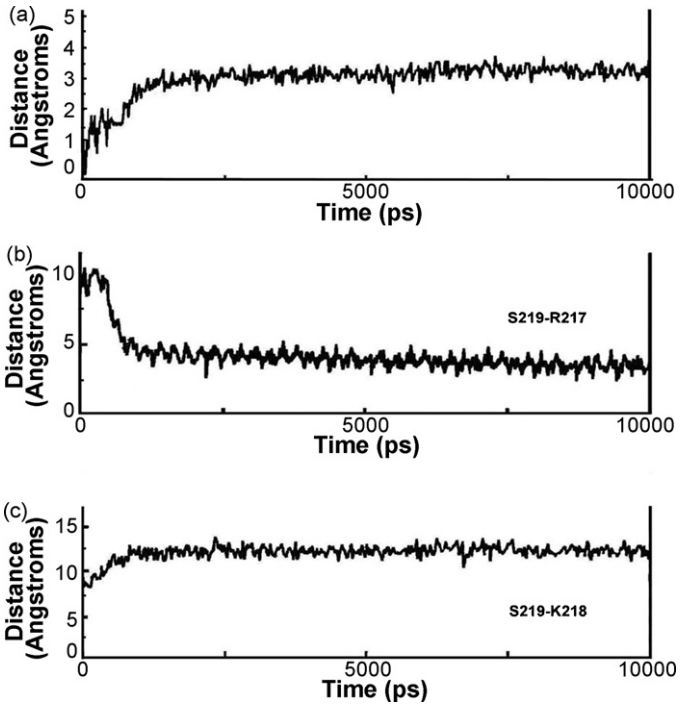

Fig. 5. The molecular dynamics simulation of ROMK1 channels. (a) Plot of the C_α root mean square deviation (RMSD) for all residues in the ROMK1 tetramer vs. simulation time. The overall RMSD for the 10 ns simulation was 3.2 Å. The plot demonstrates the structural stability of the model over the entire 10,000 ps simulation run. (b) and (c) The distance between S219 and R217 or S219 and K218 calculated over the simulation. The range for the distance between S219 and R217 is approximately 3–5 Å and that between S219 and K218 is around 11–13 Å after PKA phosphorylation.

causes enhancement of the channel-PIP_2 interaction in the pH_i gating of ROMK1 channels. The affinity of the PIP_2-channel interaction was changed in response to different pH_i values. At pH_i 6.8, the ROMK1 channel was inhibited by application of anti-PIP_2 antibodies with a $t_{1/2}$ of 44 ± 3 s (n = 5), significantly faster than at pH_i 7.4 ($t_{1/2}$ = 60.5 ± 3 s, n = 4, $P < 0.05$; Fig. 6f).

In Fig. 7a and b, the structural changes in the vicinity of the PKA phosphorylation sites before and after phosphorylation of S219 are compared. It is clearly observed that the new interaction formed by R217 and S219 brings these two residues much closer towards each other. In particular, this new interaction may result in distortion of the main chain and a more obvious movement of the K218 side chain from the PIP_2-channel interaction plane towards the cell membrane, causing the distance to become shorter from 13.8 to 7.2 Å (Fig. 7b and Table 1). This thus may increase the binding between PIP_2 and the channel, and such increase in affinity or in accessibility should account for the easier condition allowing PIP_2 to re-open the closed ROMK1 channels after PKA-phosphorylation (Fig. 6).

4. Discussion

Our present study demonstrated that PKA-mediated phosphorylation decreases the sensitivity of ROMK1 channels to pH_i and that the mutation of PKA phosphorylation sites in the C-terminal domains (S219A, S219D, S313A and S313D) shifts pK_a to an alkaline direction. PIP_2 should be involved in this process. Under the acidic condition, the affinity of PIP_2 for PKA-phosphorylated ROMK1 channels was increased as compared with those of non-phosphorylated channels (Fig. 6a). PIP_2 dose-dependently reactivated acidification-induced rundown ROMK1 channels only in those channels that had been phosphorylated by PKA. Without pretreatment with PKA catalytic subunit and ATP[γS], PIP_2 could not recover the pH_i-inhibited channels (Fig. 6). These results imply a sequence for the regulation of the pH_i gating of ROMK1 channels by PKA-mediated phosphorylation, which enhances the channel–PIP_2 interaction.

It has been suggested that Kir channels have a "TM pore" formed by the pore-loop and two TM segments and a "cytoplasmic pore" formed by the cytoplasmic N- and C-terminus. The latter forms the binding sites for ligands and for other regulators, and thereby controls the ligands to access the TM pore [37]. The binding of PIP_2 to the cytoplasmic region stabilizes the TM2 helices in an open conformation [37,38]. The PKA phosphorylation sites of ROMK1 channels on the N- and C-terminal regions modulate channel activity by different mechanisms. The phosphorylation sites on the C-terminus (S219 and S313) control the open probability of the channel by regulating the stability of the open state [36], whereas those on the N-terminus (S44) determines the number of conducting channels by masking endoplasmic reticulum retention signal [39]. Our results revealed that the mutation of S219 and S313 to alanine or aspartate in the C-terminal domains (S219A, S219D, S313A and S313D) can alter pH_i gating (Fig. 3), implying the possibility that PKA phosphorylation of ROMK1 channels mediates their pH_i gating in relation with structural changes in C-terminus. Similar findings were also reported in PKA-regulated ROMK1 channels for the enhancement of the PIP_2–channel interaction. The PKA-induced increase in affinity of the C-terminal domains for PIP_2 may require a conformational change in ROMK1 channels [23].

Table 1
Comparison of the distance and energy between residues at the phosphorylation site before and after MD simulations

	Distance between residues (Å)		Distance to the putative membrane (Å)			Total energy (kcal/mol)	Energy change (kcal/mol) ($\Delta E = {}^{*}E_{after} - {}^{**}E_{before}$)
	S219-K218	S219-R217	R217	K218	S219		
Model containing phosphate group *before* MD simulations							
	7.5	10.2	13.1	13.8	19.8	581.34	
Model containing phosphate group *after* MD simulations							
Model 1	7.8	9.8	14.1	12.2	18.1	561.45	−19.89
Model 2	7.9	9.9	14.2	12.0	18.2	562.36	−18.98
Model 3	8.2	9.1	14.8	11.3	18.5	551.85	−29.49
Model 4	13.0	3.5	15.3	10.2	17.1	583.14	1.8
Model 5	12.0	5.1	15.4	8.7	18.5	521.20	−60.14
Model 6	11.5	4.2	16.2	7.2	18.7	501.20	−80.14

The phosphate group was manually added into the system to allow the simulation to be performed. As described in Fig. 5b, the distance indicated in this table was measured between the residue tips and between the residue tip and the C_α atom of the aromatic belt (W69, W77, Y79, and W92) of the putative membrane. ${}^{*}E_{after}$ is representative of the total energy of the model containing phosphate group after MD simulations. ${}^{**}E_{before}$ is representative of the total energy of the model containing phosphate group before MD simulations.

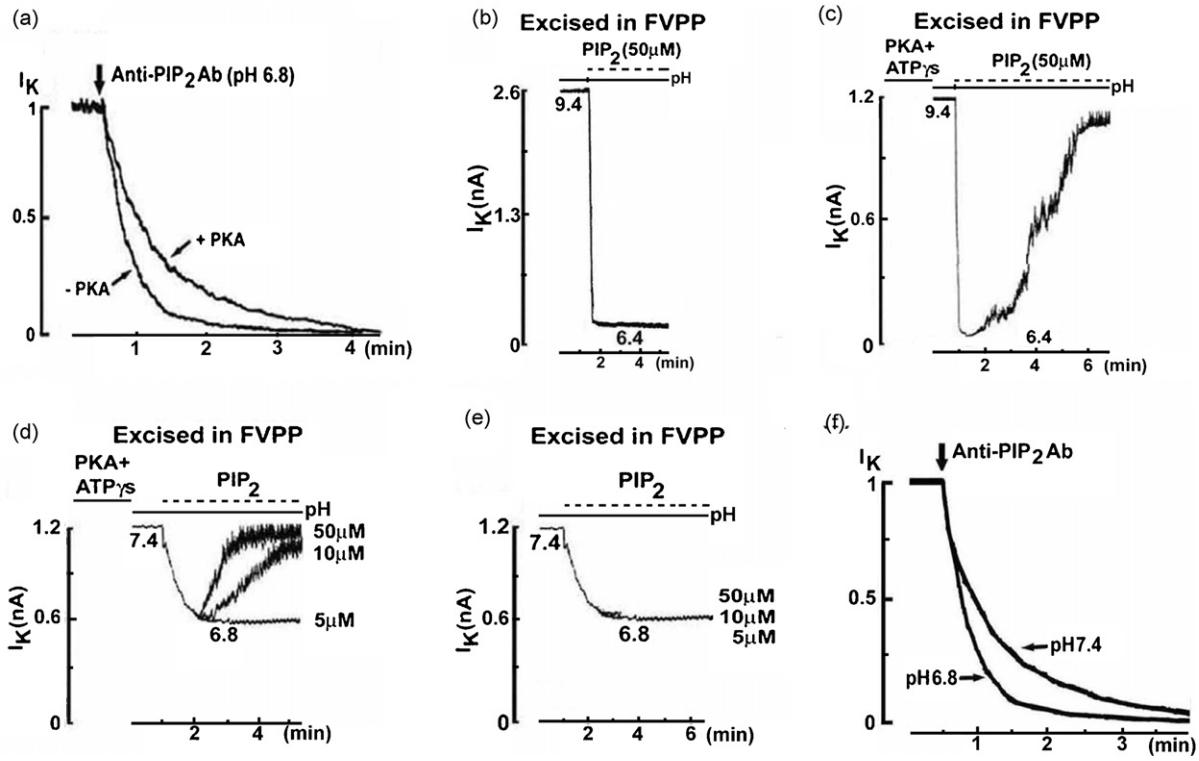

Fig. 6. The sequence effects of PKA-mediated phosphorylation and the PIP_2-channel interaction on pH_i gating. (a) At pH_i 6.8, the inhibition of ROMK1 channels by application of anti-PIP_2 antibodies is significantly faster than by PKA-phosphorylation ($t_{1/2}$ = 45 ± 3 s vs. 60 ± 3 s, n = 4, $P < 0.05$). (b) PIP_2 (50 μM) alone cannot recover ROMK1 channel currents during the rapid acidification (from pH_i 9.4 to 6.4). (c) ROMK1 channels were pre-treated with PKA catalytic subunit (100 units/ml) and ATP[γS] (0.5 mM) for 5 min, the acidification (pH_i 9.4–6.4)-caused inhibition was fully recovered by 50 μM PIP_2. (d) The pH_i (pH_i 7.4–6.8)-induced inhibition of ROMK1 channels was overcome by PIP_2 in a dose-dependent manner only in the presence of PKA-mediated phosphorylation. Both 10 and 50 μM (but not 5 μM) PIP_2 completely reactivated the rundown channels. (e) Without pretreatment with PKA catalytic subunit and ATP[γS], none of the three concentrations of PIP_2 reactivated rundown channels. (f) The affinity of the PIP_2–channel interaction was changed in response to different pH_i values ($t_{1/2}$ = 44 ± 3 s at pH_i 6.8 vs. 60.5 ± 3 s at pH_i 7.4, n = 4, $P < 0.05$).

Homology models of ROMK1 channels based on the crystal structure of the closely related bacterial Kir channel KirBac1.1 [21] provides guidance on the pathway of PKA-mediated phosphorylation that affects pH_i sensitivity. In our homology model of the ROMK1 channel, a PKA phosphorylation site (S219) was spatially close to the PIP_2 binding residues (R188, R217, and K218) (Fig. 4c). The MD simulation provides supplementary but critical knowledge to have better understanding on the behavior of cytoplasmic domains in the ligand-free form, for which no structural information is available [19,40]. Our MD simulation results showed that PKA-mediated phosphorylation of the ROMK1 channel leads to a conformational change in the C-terminus. A fascinating finding after PKA phosphorylation is the shortening of the distance between S219 and R217 and the pulling of K218 toward the membrane (Fig. 5 and Table 1). Similar findings were also reported for the PKA-mediated phosphorylation in the N-terminal domains of the regulatory light chain of smooth muscle myosin with MD simulations. In that case, after PKA phosphorylation, the distance between a S19 residue and an R16 residue is shortened on the regulatory light chain. This conformational change ultimately activates the myosin interaction with actin [41]. Our results suggest that PKA-mediated phosphorylation draws the PIP_2 binding motif from its original position towards the membrane, and this stabilizes the open state of the ROMK1 channel in response to change in intracellular proton levels. This hypothesis needs to be examined by X-ray crystal structure studies in the future.

We propose a molecular mechanism to describe the structural details of pH_i-sensitive channel gating regulated by PKA-mediated phosphorylation in ROMK1 channels (Fig. 7c). At pH_i 6.4, which is below the pK_a (~6.9), the ROMK1 channel is normally closed. The channels enter a nonconductive state subsequent to pH_i inhibition [42]. In the absence of phosphorylation by PKA, PIP_2 is unable to re-open the channel. When PKA-mediated phosphorylation occurs upon using ATP[γS] as substrate [33], which does not generate PIP_2 [23], the conformational change resulting from phosphorylation causes the cytoplasmic pore to open to a certain extent, but not sufficient for full recovery of the pH_i-induced closure. When PIP_2 is generated using MgATP as substrate [15], PKA-mediated phosphorylation results in the pulling of the PIP_2-binding regions towards the membrane, and thus fix the channel to go back to the open state. The reactivation of ROMK1 channels by PIP_2 may correspond to a relative effective and required conformational change [43,38]. Therefore, in this way, the ROMK1 channels can be re-opened by PKA catalytic subunit and Mg-ATP from pH_i inhibition, even at pH_i 6.4.

A previous study with MD simulations suggested that the structural arrangement of the C-terminus might determine the opening and closing of Kir 3.1 and Kir 6.2 channels [40]. In addition, several research groups have reported that, in the simulation results for Kir 1.1, Kir 3.1, Kir 6.2, and KcsA channels, the motions in the conformational space and stability for channel structures can be represented by a 10 ns timescale [19,40,44]. However, from a purely statistical point of view, it is clearly understood that such simulations (~10 ns) should not be able to fully sample the motions of a protein in question [45]. Nevertheless, we found that PKA-mediated phosphorylation did induce changes in the RMSD

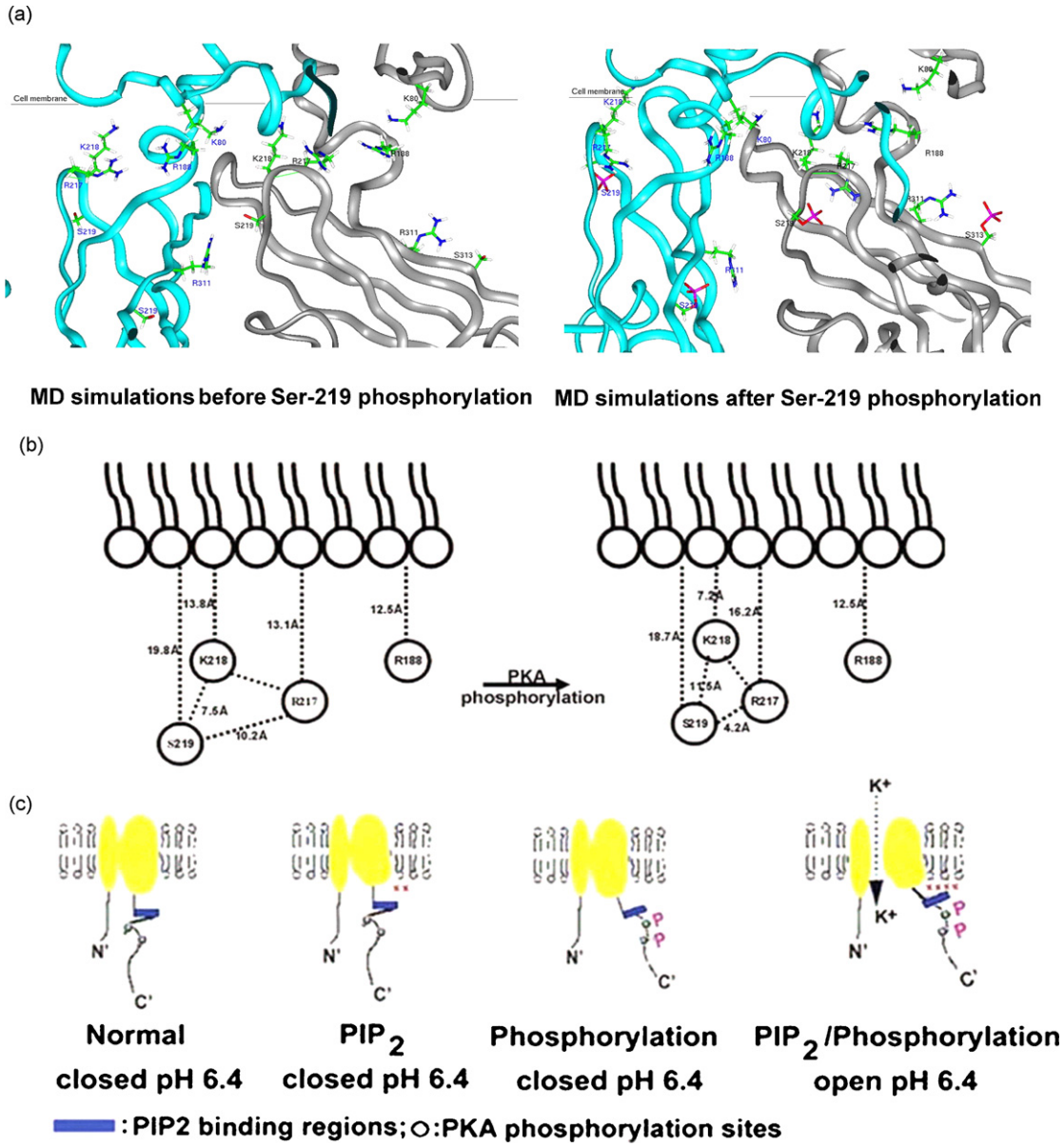

Fig. 7. Working model for the pH_i sensitivity of ROMK1 channels mediated by PIP_2 and PKA. (a) The stereo diagrams of the vicinity of the PKA phosphorylation site with (right) or without (left) phosphorylation of S219. The main chains of adjacent subunits are represented as gray and blue ribbons. It is clearly seen that the new interaction formed by R217 and S219 brings these two residues much closer together after phosphorylation. In particular, this new interaction may result in distortion of the main chain and a more obvious movement of the K218 side chain from the PIP_2–channel interaction plane towards the cell membrane, which thus increases the binding between PIP_2 and the channel. (b) Cartoon showing the distances between R217, K218, as well as S219 and the putative membrane. Distances were obtained through MD simulations. (c) Schematic diagrams describing the regulation of PIP_2 binding residues and PKA phosphorylation sites in pH_i gating of ROMK1 channels.

and in distances between residues (Fig. 5). All those MD simulation reached equilibrium after 3 ns. Therefore, the structure model presented here may at least reflect a fairly stable transition state after phosphorylation in ROMK1 channels. Our data identify that a PKA phosphorylation site, S219, should induce conformational changes to regulate pH_i-dependent channel gating. The mutation of S219 observed in HPS/aBS has been shifted to more alkaline pH values [15,16]. In the present study, we have elucidated a potential molecular mechanism.

In conclusion, the pH_i gating is believed to act as a physiological feedback mechanism that prevents excessive loss of K^+ during metabolic acidosis. Our findings provide a new mechanistic insight into the sequence role of PKA-mediated phosphorylation in regulating the pH_i sensitivity of ROMK1 channels. The elucidation of the molecular mechanisms of PKA and pH_i gating will be instrumental in discovering ways to treat HPS/aBS.

Acknowledgements

We thank Dr. Chou-Long Huang (Department of Medicine, University of Texas Southwestern Medical Center, Dallas) for kindly providing the ROMK1 channel cDNA and for his critical reading of the manuscript. We also thank Prof. Roderick MacKinnon (Howard Hughes Medical Institute, Laboratory of Molecular Neurobiology and Biophysics, Rockefeller University) for valuable comments. This work was supported by grants from the National Science Council (93-2320-B-002-028 and 94-2320-B-002-112), Taipei, Taiwan. The authors are also very grateful to Dr. Pao-Hsiang

Wang for his enthusiastic and invaluable help in the correction of the manuscript.

References

[1] C.G. Nichols, A.N. Lopatin, Inward rectifier potassium channels, Annu. Rev. Physiol. 59 (1997) 171–191.
[2] S.C. Hebert, G. Desir, G. Giebisch, W. Wang, Molecular diversity and regulation of renal potassium channels, Physiol. Rev. 85 (2005) 319–371.
[3] K. Ho, C.G. Nichols, W.J. Lederer, J. Lytton, P.M. Vassilev, M.V. Kanazirska, S.C. Hebert, Cloning and expression of an inwardly rectifying ATP-regulated potassium channel, Nature 362 (1993) 31–38.
[4] N.M. Plaster, R. Tawil, M. Tristani-Firouzi, S. Canun, S. Bendahhou, A. Tsunoda, M.R. Donaldson, S.T. Iannaccone, E. Brunt, R. Barohn, J. Clark, F. Deymeer, A.L. George Jr., F.A. Fish, A. Hahn, A. Nitu, C. Ozdemir, P. Serdaroglu, S.H. Subramony, G. Wolfe, Y.H. Fu, L.J. Ptacek, Mutations in Kir2.1 cause the developmental and episodic electrical phenotypes of Andersen's syndrome, Cell 105 (2001) 511–519.
[5] S. Signorini, Y.J. Liao, S.A. Duncan, L.Y. Jan, M. Stoffel, Normal cerebellar development but susceptibility to seizures in mice lacking G protein-coupled, inwardly rectifying K^+ channel GIRK2, Proc. Natl. Acad. Sci. U.S.A. 94 (1997) 923–927.
[6] K. Wickman, J. Nemec, S.J. Gendler, D.E. Clapham, Abnormal heart rate regulation in GIRK4 knockout mice, Neuron 20 (1998) 103–114.
[7] M. Peters, N. Jeck, S. Reinalter, A. Leonhardt, B. Tonshoff, G.G. Klaus, M. Konrad, H.W. Seyberth, Clinical presentation of genetically defined patients with hypokalemic salt-losing tubulopathies, Am. J. Med. 112 (2002) 183–190.
[8] C. Derst, M. Konrad, A. Kockerling, L. Karolyi, G. Deschenes, J. Daut, A. Karschin, H.W. Seyberth, Mutations in the ROMK gene in antenatal Bartter syndrome are associated with impaired K^+ channel function, Biochem. Biophys. Res. Commun. 230 (1997) 641–645.
[9] U. Schulte, H. Hahn, M. Konrad, N. Jeck, C. Derst, K. Wild, S. Weidemann, J.P. Ruppersberg, B. Fakler, J. Ludwig, pH gating of ROMK (Kir1.1) channels: control by an Arg-Lys-Arg triad disrupted in antenatal Bartter syndrome, Proc. Natl. Acad. Sci. U.S.A. 96 (1999) 15298–15303.
[10] C. Jiang, Z. Qu, H. Xu, Gating of inward rectifier K^+ channels by proton-mediated interactions of intracellular protein domains, Trends Cardiovasc. Med. 12 (2002) 5–13.
[11] S. Chanchevalap, Z. Yang, N. Cui, Z. Qu, G. Zhu, C. Liu, L.R. Giwa, L. Abdulkadir, C. Jiang, Involvement of histidine residues in proton sensing of ROMK1 channel, J. Biol. Chem. 275 (2000) 7811–7817.
[12] Q. Leng, G.G. MacGregor, K. Dong, G. Giebisch, S.C. Hebert, Subunit-subunit interactions are critical for proton sensitivity of ROMK: evidence in support of an intermolecular gating mechanism, Proc. Natl. Acad. Sci. U.S.A. 103 (2006) 1982–1987.
[13] T.P. Flagg, D. Yoo, C.M. Sciortino, M. Tate, M.F. Romero, P.A. Welling, Molecular mechanism of a COOH-terminal gating determinant in the ROMK channel revealed by a Bartter's disease mutation, J. Physiol. 544 (2002) 351–362.
[14] Z.C. Xu, Y. Yang, S.C. Hebert, Phosphorylation of the ATP-sensitive, inwardly rectifying K^+ channel, ROMK, by cyclic AMP-dependent protein kinase, J. Biol. Chem. 271 (1996) 9313–9319.
[15] U. Schulte, B. Fakler, Gating of inward-rectifier K^+ channels by intracellular pH, Eur. J. Biochem. 267 (2000) 5837–5841.
[16] P.G. Starremans, A.W. van der Kemp, N.V. Knoers, L.P. van den Heuvel, R.J. Bindels, Functional implications of mutations in the human renal outer medullary potassium channel (ROMK2) identified in Bartter syndrome, Pflugers. Arch. 443 (2002) 466–472.
[17] J. Leipziger, G.G. MacGregor, G.J. Cooper, J. Xu, S.C. Hebert, G. Giebisch, PKA site mutations of ROMK2 channels shift the pH dependence to more alkaline values, Am. J. Physiol. 279 (2000) F919–926.
[18] P. Beguin, K. Nagashima, M. Nishimura, T. Gonoi, S. Seino, PKA-mediated phosphorylation of the human K(ATP) channel: separate roles of Kir6.2 and SUR1 subunit phosphorylation, EMBO J. 18 (1999) 4722–4732.
[19] S. Haider, S. Khalid, S.J. Tucker, F.M. Ashcroft, M.S. Sansom, Molecular dynamics simulations of inwardly rectifying (Kir) potassium channels: a comparative study, Biochemistry 46 (2007) 3643–3652.
[20] R.J. Law, R.H. Henchman, J.A. McCammon, A gating mechanism proposed from a simulation of a human alpha7 nicotinic acetylcholine receptor, Proc. Natl. Acad. Sci. U.S.A. 102 (2005) 6813–6818.
[21] A. Kuo, J.M. Gulbis, J.F. Antcliff, T. Rahman, E.D. Lowe, J. Zimmer, J. Cuthbertson, F.M. Ashcroft, T. Ezaki, D.A. Doyle, Crystal structure of the potassium channel KirBac1.1 in the closed state, Science 300 (2003) 1922–1926.
[22] C.L. Huang, S. Feng, D.W. Hilgemann, Direct activation of inward rectifier potassium channels by PIP_2 and its stabilization by Gbetagamma, Nature 391 (1998) 803–806.
[23] H.H. Liou, S.S. Zhou, C.L. Huang, Regulation of ROMK1 channel by protein kinase A via a phosphatidylinositol 4,5-bisphosphate-dependent mechanism, Proc. Natl. Acad. Sci. U.S.A. 96 (1999) 5820–5825.
[24] P. Proks, C.E. Capener, P. Jones, F.M. Ashcroft, Mutations within the P-loop of Kir6.2 modulate the intraburst kinetics of the ATP-sensitive potassium channel, J. Gen. Physiol. 118 (2001) 341–353.
[25] Y.M. Leung, W.Z. Zeng, H.H. Liou, C.R. Solaro, C.L. Huang, Phosphatidylinositol 4,5-bisphosphate and intracellular pH regulate the ROMK1 potassium channel via separate but interrelated mechanisms, J. Biol. Chem. 275 (2000) 10182–10189.
[26] P.T. Huang, T.Y. Chen, L.J. Tseng, K.L. Lou, H.H. Liou, T.B. Lin, H.C. Spatz, Y.Y. Shiau, Structural influence of hanatoxin binding on the carboxyl terminus of S3 segment in voltage-gated K^+-channel Kv2.1, Receptors Channels 8 (2002) 79–85.
[27] K.L. Lou, P.T. Huang, Y.S. Shiau, Y.C. Liaw, Y.Y. Shiau, H.H. Liou, A possible molecular mechanism of hanatoxin binding-modified gating in voltage-gated K^+-channels, J. Mol. Recognit. 16 (2003) 392–395.
[28] Y.S. Shiau, P.T. Huang, H.H. Liou, Y.C. Liaw, Y.Y. Shiau, K.L. Lou, Structural basis of binding and inhibition of novel tarantula toxins in mammalian voltage-dependent potassium channels, Chem. Res. Toxicol. 16 (2003) 1217–1225.
[29] V.Z. Spassov, L. Yan, S. Szalma, Introducing an implicit membrane in generalized born/solvent accessibility continuum solvent, J. Phys. Chem. B 106 (2002) 8726–8738.
[30] T.A. Darden, L.G. Pedersen, Molecular modeling: an experimental tool, Environ. Health Perspect. 101 (1993) 410–412.
[31] B. Hess, H. Bekker, H.J.C. Berendsen, J.G.E.M. Fraaije, LINCS: a linear constraint solver for molecular simulations, J. Comput. Chem. 18 (1997) 1463–1472.
[32] D.W. Hilgemann, R. Ball, Regulation of cardiac Na^+, Ca^{2+} exchange and KATP potassium channels by PIP_2, Science 273 (1996) 956–959.
[33] F. Eckstein, Nucleoside phosphorothioates, Annu. Rev. Biochem. 54 (1985) 367–402.
[34] H. Choe, H. Zhou, L.G. Palmer, H. Sackin, A conserved cytoplasmic region of ROMK modulates pH sensitivity, conductance, and gating, Am. J. Physiol. 273 (1997) F16–F29.
[35] B. Fakler, J.H. Schultz, J. Yang, U. Schulte, U. Brandle, H.P. Zenner, L.Y. Jan, J.P. Ruppersberg, Identification of a titratable lysine residue that determines sensitivity of kidney potassium channels (ROMK) to intracellular pH, EMBO J. 15 (1996) 4093–4099.
[36] G.G. MacGregor, J.Z. Xu, C.M. McNicholas, G. Giebisch, S.C. Hebert, Partially active channels produced by PKA site mutation of the cloned renal K^+ channel, ROMK2 (Kir1.2), Am. J. Physiol. 275 (1998) F415–F422.
[37] L.H. Xie, S.A. John, B. Ribalet, J.N. Weiss, Activation of inwardly rectifying potassium (Kir) channels by phosphatidylinosital-4,5-bisphosphate (PIP_2): interaction with other regulatory ligands, Prog. Biophys. Mol. Biol. 94 (2007) 320–335.
[38] J. Xiao, X.G. Zhen, J. Yang, Localization of PIP_2 activation gate in inward rectifier K^+ channels, Nat. Neurosci. 6 (2003) 811–818.
[39] A.D. O'Connell, Q. Leng, K. Dong, G.G. MacGregor, G. Giebisch, S.C. Hebert, Phosphorylation-regulated endoplasmic reticulum retention signal in the renal outer-medullary K^+ channel (ROMK), Proc. Natl. Acad. Sci. U.S.A. 102 (2005) 9954–9959.
[40] S. Haider, A. Grottesi, B.A. Hall, F.M. Ashcroft, M.S. Sansom, Conformational dynamics of the ligand-binding domain of inward rectifier K channels as revealed by molecular dynamics simulations: toward an understanding of Kir channel gating, Biophys. J. 88 (2005) 3310–3320.
[41] L.M. Espinoza-Fonseca, D. Kast, D.D. Thomas, Molecular dynamics simulations reveal a disorder-to-order transition on phosphorylation of smooth muscle myosin, Biophys. J. 93 (2007) 2083–2090.
[42] A. Dahlmann, M. Li, Z. Gao, D. McGarrigle, H. Sackin, L.G. Palmer, Regulation of Kir channels by intracellular pH and extracellular K^+: mechanisms of coupling, J. Gen. Physiol. 123 (2004) 441–454.
[43] D.A. Doyle, J.C. Morais, R.A. Pfuetzner, A. Kuo, J.M. Gulbis, S.L. Cohen, B.T. Chait, R. MacKinnon, The structure of the potassium channel: molecular basis of K^+ conduction and selectivity, Science 280 (1998) 69–77.
[44] C.E. Capener, P. Proks, F.M. Ashcroft, M.S. Sansom, Filter flexibility in a mammalian K channel: models and simulations of Kir6.2 mutants, Biophys. J. 84 (2003) 234–236.
[45] J.D. Faraldo-Gomez, L.R. Forrest, M. Baaden, P.J. Bond, C. Domene, G. Patargias, J. Cuthbertson, M.S. Sansom, Conformational sampling and dynamics of membrane proteins from 10-nanosecond computer simulations, Proteins 57 (2004) 783–791.